Biosensors and Bioelectronics 31 (2012) 343–348

Contents lists available at SciVerse ScienceDirect

Biosensors and Bioelectronics

journal homepage: www.elsevier.com/locate/bios

A CMOS label-free DNA sensor using electrostatic induction of molecular charges

Kang-Ho Lee, Jeong Oen Lee, Sukhwan Choi, Jun-Bo Yoon, Gyu-Hyeong Cho*

School of EECS, Korea Advanced Institute of Science and Technology, 335, Gwahakro, Yuseong-gu, Daejeon, 305-701, South Korea

ARTICLE INFO

Article history:
Received 30 August 2011
Received in revised form 21 October 2011
Accepted 21 October 2011
Available online 28 October 2011

Keywords:
DNA hybridization
Negative charge
FET sensor
Accumulation

ABSTRACT

This paper reports a label-free biosensor for the detection of DNA hybridization. The proposed biosensor measures the surface potential on oligonucleotide modified electrodes using a direct charge accumulation method. The sensor directly and repeatedly measures the charges induced in the working electrode, which correspond to intrinsic negative charges in immobilized molecules. The sensor achieves an improved signal-to-noise ratio (SNR), through the oversampling effect of accumulation for charges and the differential architecture. The sensor also shows stable, robust, and reproducible measurement independent of slight changes in the reference voltage, unlike previous ion-sensitive field effect transistors (ISFETs), providing the benefits of choosing a wide variety of reference electrode materials. The proposed device is integrated with working electrodes, a reference electrode and readout circuits into one package via a 0.35 μm complementary metal-oxide-semiconductor (CMOS) process. The sensor achieves a detectable range of 88.3 dB and a detection limit of 36 μV for surface potential. It is demonstrated that the sensor successfully achieves specific detection of oligonucleotide sequences derived from the H5N1 avian influenza virus. The experiments show a limit of detection of 100 pM and include a single-base mismatch test in 18-mer oligonucleotides.

1. Introduction

DNA sensors are important in diagnostic tests for genomics studies and in early cancer detection and drug discovery (Moore, 2001). Most DNA hybridization detection techniques require the attachment of target molecules, such as fluorescent, chemiluminescent or redox labels (Boon et al., 2002; Kricka, 1999). However, these techniques are costly, time-consuming and relatively bulky for portable devices. Recently developed silicon devices based on field-effect phenomena offer label-free and direct electrical detection when used to quantify the hybridization of DNA molecules. This results in rapid, robust, and inexpensive measurement and compatibility with commercial microfabrication technology (Stern et al., 2007; Elfstrom et al., 2008). With respect to field-effect device, ion-sensitive field effect transistors (ISFETs) have demonstrated the capability to detect net surface charges via the intrinsic negative charge in immobilized molecules through a shift of the threshold voltage or a change in the drain current (Bergveld, 1970; Kim et al., 2004). However, these technologies are substantially affected by the conversion efficiency in the charge density at the semiconductor space–charge region corresponding to the net surface charge at the electrolyte–electrode interface (Lee et al., 2009). The ion-sensitive region at the gate of the transistor is limited in terms of area for bio-modification due to the non-uniformity of the oxide thickness. These devices are also limited by their minimum detectable level (several mV) of the surface charge, because small fluctuating signals are buried by the noise components of the FET (Sawada et al., 2004; Poghossian et al., 2005). The main drawback associated with ISFETs is the need for reference electrodes (usually made of Ag/AgCl) which cannot be easily integrated in a standard CMOS process, thus preventing the realization of low-cost and miniaturized devices. These devices require a fixed voltage that is applied accurately via a reference electrode to determine the potential of the analyte solution. Slight changes in the reference voltage can cause a decline in the performance of the sensor when used in conjunction with floating gate-biasing structures such as ISFETs. Thus, these devices must be used with stable and reproducible standard electrodes (Ag/AgCl) (Souteyrand et al., 1997; Fritz et al., 2002) or pseudo electrodes (Ag or Pt wire) (Perkins et al., 2002; Berney et al., 2000), which require additional fabrication processes.

In this paper, we propose a method that directly and repeatedly measures the charges that correspond to the changes in the surface potential, thus improving the signal-to-noise ratio (SNR) through an oversampling effect by accumulation using active components. The proposed device, which measures the net surface potential directly, is independent of the uniformity of the gate oxide. As a result, the bio-modified region of the electrodes can be extended beyond that of previous works (Bergveld, 1970; Kim et al., 2004), allowing an increase in the level of the detectable signal per instance of the signal. The reference electrode in our device

* Corresponding author. Tel.: +82 42 350 3424; fax: +82 42 350 8024.
E-mail address: ghcho@ee.kaist.ac.kr (G.-H. Cho).

0956-5663/$ – see front matter © 2011 Elsevier B.V. All rights reserved.
doi:10.1016/j.bios.2011.10.042

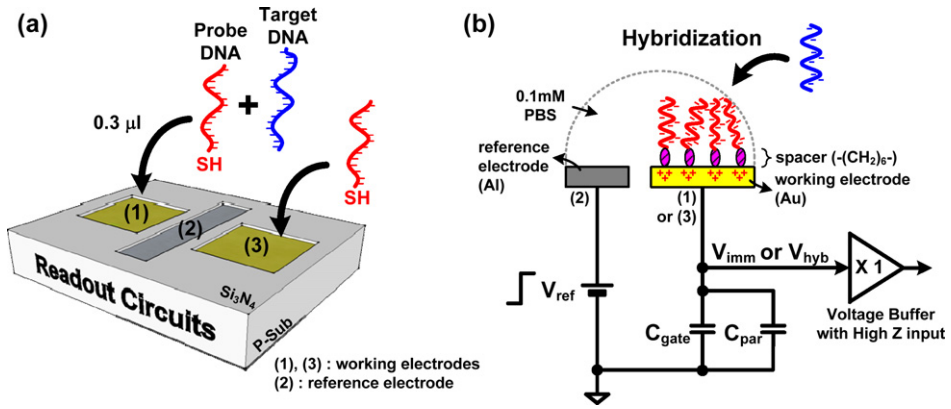

Fig. 1. (a) A conceptual view of the proposed device. The built-in electrodes are composed of working electrodes (Au, (1) and (3)) modified with DNA strands and a reference electrode (Al, (2)) that determines the potential of the analyte solution. (b) The working principle with a first-order model. The induced potential in the working electrodes is V_{imm} (functionalized with the only probe DNA strands) or V_{hyb} (after hybridization of the target DNA). The input of the voltage buffer circuit is modeled with the gate capacitance C_{gate} of a MOSFET and the parasitic capacitance C_{par}.

is integrated with working electrodes and readout circuits into one package. The device achieved stable operation despite wide variation of the reference voltage due to its differential structure and direct sensing of the surface charge. Thus, we could use naked aluminum exposed in a standard CMOS fabrication process as the material of the reference electrode, eliminating the additional fabrication cost and providing large-scale-of-integration capabilities.

The proposed sensor is demonstrated to achieve the specific detection of oligonucleotide sequences derived from the H5N1 avian influenza virus (Pipper et al., 2007).

2. Methods

2.1. Device structure and first-order model

The proposed device includes metal electrodes and readout circuits on a silicon substrate. The electrodes, which are exposed to the analyte solution, are built into the top surface of a *p*-type substrate. Readout circuits are located below the substrate, interfacing with the metal electrodes and the external device.

Fig. 1(a) shows a conceptual view of the proposed device. The built-in electrodes are working electrodes that are modified with DNA strands and a reference electrode that determines the potential of the analyte solution. Silicon nitride (Si_3N_4) isolates and protects readout circuits from the electrolyte solution. The differential architecture in this device, which detects the relative difference in the surface potential between the only probe-functionalized working electrode and the hybridized working electrode, excludes common disturbing or interfering noise such as thermal fluctuations, drifts, non-specific binding, and changes in the electrolyte composition, thus enabling accurate measurement (Fritz et al., 2002). The device uses gold (Au) as the material for the working electrodes, as gold binds strongly to organic molecules containing a thiol group. Aluminum (Al) is used for the reference electrode. In previous works, electrodes composed of a specified material, usually Ag/AgCl, were crucial as a floating reference electrode. This limitation regarding electrode selection necessitates an additional fabrication process, resulting in difficulties associated with integration. Our device can stably obtain a potential change of the surface charge regardless of the electrode material (see Fig. 5(b) in Section 3). In this study, we used Al as a reference electrode because Al is a naked metal that is exposed after a standard pad opening operation during passivation fabrication.

Fig. 1(b) shows the working principle of this device, simplified with a first-order model. This sensor is based on the electrostatic laws of induction and designed to detect the negative electric charge associated with oligonucleotides. In other words, an active area functionalized with a proper sandwich of a spacer ($(Ch_2)_6$) and single-strand oligonucleotides is constructed on the surface of the electrodes to provide the charge Q_i which is induced by the electric field generated by the sensing charge Q_s of oligonucleotides. The induced working electrodes are connected to the voltage buffer circuit which has input characteristics of high impedance: no charges flow through any path in the steady state. The input of the voltage buffer circuit can be modeled equivalently with the gate capacitance C_{gate} of the MOS (metal-oxide semiconductor) transistor and the parasitic capacitance C_{par}. The reference voltage, V_{ref}, is used to set the operating point of the voltage buffer circuit through the electrolyte solution.

The relationship between the surface charge Q_s and the voltage of the high impedance node, V_{imm} or V_{hyb}, follows the charge conservation principle which states that the total charge into the high impedance node must remain constant. Writing all charges in terms of capacitances, we obtain the following equations:

$$Q_i(Q_{imm}) + (C_{par} + C_{gats})V_{imm} = Q_i(Q_{hyb}) + (C_{par} + C_{gats})V_{hyb} \quad (1)$$

$$\Delta V = (V_{hyb} - V_{imm}) = \frac{Q_i(Q_{imm}) - Q_i(Q_{hyb})}{C_{par} + C_{gate}} \quad (2)$$

Here, $Q_i(Q_{imm})$ is the charge induced on the working electrode by the surface charge Q_{imm} after immobilization of the probe DNA, while $Q_i(Q_{hyb})$ is the charge induced after hybridization of the probe and target DNA. V_{imm} is voltage generated by the immobilization of the probe DNA and V_{hyb} denotes the voltage after hybridization of the DNA strands. Eq. (2) expresses that the voltage change arises after hybridization of the DNA strands resulting from changes in the surface potential. Here, a first-order model simplification suggests that a hypothesis of perfect induction is plausible if the spacer thickness is much thinner than other dimensions. In this case, the induced charge $Q_i(Q_{imm})$ or $Q_i(Q_{hyb})$ would be equal in magnitude and opposite in sign to the sensing charge Q_{imm} or Q_{hyb}, respectively; that is,

$$Q_i(Q_{imm}) = -Q_{imm} \quad (3)$$

$$Q_i(Q_{hyb}) = -Q_{hyb} \quad (4)$$

Using Eqs. (3) and (4), the effective change in the surface potential observed after hybridization of the DNA strands can be expressed as

$$\Delta V = \frac{Q_{hyb} - Q_{imm}}{C_{par} + C_{gate}}, \qquad C_{gate} = C_{gb} + C_{gd} + C_{gs}$$

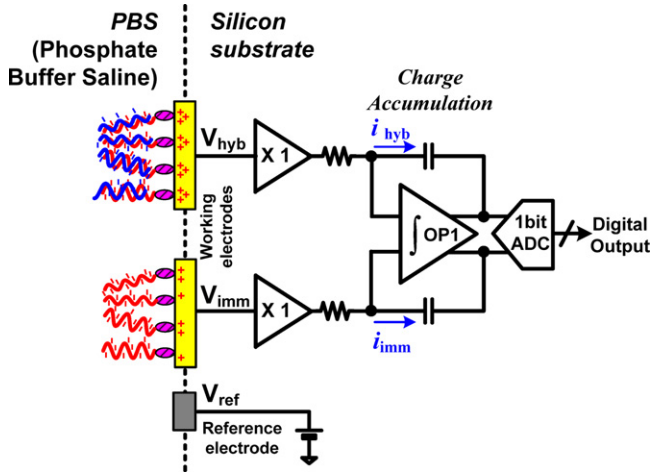

Fig. 2. Simplified description of the readout circuits. The readout circuits are composed of a voltage buffer circuit, an integrator, and a one-bit analog-to-digital converter (ADC). The charges induced in the working electrodes are transferred to the integrator through the voltage buffer circuit. They are then accumulated and digitalized.

where C_{gb}, C_{gd} and C_{gs} are the capacitances that exist from the gate to the substrate body, the drain and the source, respectively.

The amount of electric charge immobilized on the surface of the electrodes modulates the voltage variation at the high impedance node of the voltage buffer circuit. These voltage changes can be measured by the following direct accumulation methods.

2.2. Design of a FET sensor using a direct accumulation method

The sensor directly measures the charges induced in the working electrode, which correspond to intrinsic negative charges in immobilized molecules. After this measurement (reading) of the signals of the binding event, it is accumulated at storage component at high speeds, while cancelling of noise components thanks to averaging effect of integrator (Lee et al., 2010). And finally, the accumulated signals output in digitized shape.

The proposed device is based on direct measurement of the surface potential, while previous works (Bergveld, 1970; Kim et al., 2004; Lee et al., 2009) depended on the movement of charge carriers in the electric field generated by the surface charge. Fig. 2 shows a simplified description of the readout circuits. The readout circuits are composed of three parts: a voltage buffer circuit, an integrator and an analog-to-digital convertor (ADC). The voltage buffer circuit has the input characteristic of high impedance due to the use of a transistor with an isolated gate. Thus, it ideally transfers charges induced in the working electrodes to the succeeding stage of the integrator without any leaky charges. The transferred signals are then accumulated by the fully differential switched-capacitor type integrator (Lee et al., 2010). The detailed schematics and operation of this integrator are shown in the Supplementary material (Figs. S-1 and 2). As the signal integration cycle is repeated, the signal charge accumulates and then, the differential information in the surface potential increases and expands the readable signals. Through this integrating operation, it is expected that the SNR of the device increases (Sawada et al., 2004).

Commonly, the resolution of the ISFET is restricted by the 1/f noise component of the transistor. Thus, the ISFET cannot normally be used to measure infinitesimal variations of the surface potential (Lee et al., 2008). Some works have attempted to improve the SNR of this device by using a charge transfer technique (Sawada et al., 2004). However, this technique is limited in terms of the number of signal integration cycles because the gate capacitance of the source follower circuit is quickly saturated by the current flowing through the device. Our device accumulates charges a number of times, which are generated corresponding to the difference in the surface potential between the two differential electrodes using an active component (OP1). In this experiment, the signal charges are accumulated within a maximum accumulation time of 170 ms at a speed of 50,000 cycles/s, resulting in significant improvement of the SNR of the device.

The accumulated signal is then transformed into a square signal and interfaced with external digital devices through a one-bit analog-to-digital converter, which is composed of a comparator, a counter, and a shift register. A block diagram illustrates this in detail in Supplementary material (Fig. S-3).

The direct sensing method in this paper measures the charges induced by surface potential without any conversion loss. The differential structure reduces common-noise and allows only the differential components in signals. In addition, the accumulation method results in an increase of SNR in the device. These characteristics improve the performance of the sensor providing the benefits of an independence of the reference voltage. In other words, although the use of aluminum instead of standard Ag/AgCl causes the voltage drop across the electrolyte solution, the devices operates properly as long as the voltage in the working electrode is within the operating range of the voltage buffer circuit. Accordingly, it offers the advantage of using a low-cost and highly integrated DNA sensor regardless of the fabrication of the specified materials unlike the conventional floating reference electrode of Ag/AgCl.

2.3. Sensor fabrication and experimental setup

Fig. 3(a) presents a prototype measurement board and a chip microphotograph of the DNA sensor as fabricated in the standard 0.35 μm CMOS process. To use Al as a reference electrode, we opened pre-defined squares in the passivation layers; in contrast, the Au for the working electrodes was fabricated using post-processing steps, as shown in Fig. 3(b). The post-processing steps are as follows: a 20 nm-thick layer of Cr was deposited as an adhesion layer between the exposed Al and the Au. A 100 nm-thick Au layer was then patterned by a lift-off process using a negative photoresist. The unit electrode has a 71 μm^2 on the surface of the sensor. The total area of the chip is 20 mm^2 and the active area of the readout circuit is 1.64 mm^2. The chip was attached to a PCB and electrically contacted using gold bonding wires. Shielding epoxy was used to protect both the bonded wires and the chip's I/O pads from contact with the saline solution. A prototype measurement board was implemented to test the designed biosensor.

2.4. DNA oligonucleotide and surface preparation

Influenza is a highly contagious respiratory infection that results in high morbidity and mortality (Werner and Harder, 2006). In this experiment, the following oligonucleotide derived from the H5N1 avian influenza virus was used: CCA AGC AAC AGA CTC AAA (Bioneer Co., Republic of Korea) (Pipper et al., 2007). Thiol-functionalized probes, which were modified with a chain of six carbon atoms as a spacer, have a sequence that is complementary to that of the oligonucleotide from H5N1. The sequence of the non-specific target used as a negative control to verify hybridization between the probe and complimentary target strands was as follows: 5′-AAC GTA CCT GTC TGT CCC-3′.

Before performing the DNA experiment, the electrodes of the device were cleaned thoroughly with acetone, methanol, and distilled water for 3 min each. After cleaning, the electrodes surfaces were activated by means of O_2 plasma treatment at 200 W for 60 s (Han et al., 2010). A layer of 10 μM DNA probes was constructed on the electrodes by incubating the surface of the chip for 6 h at room temperature. After a probe immobilization step, the surface

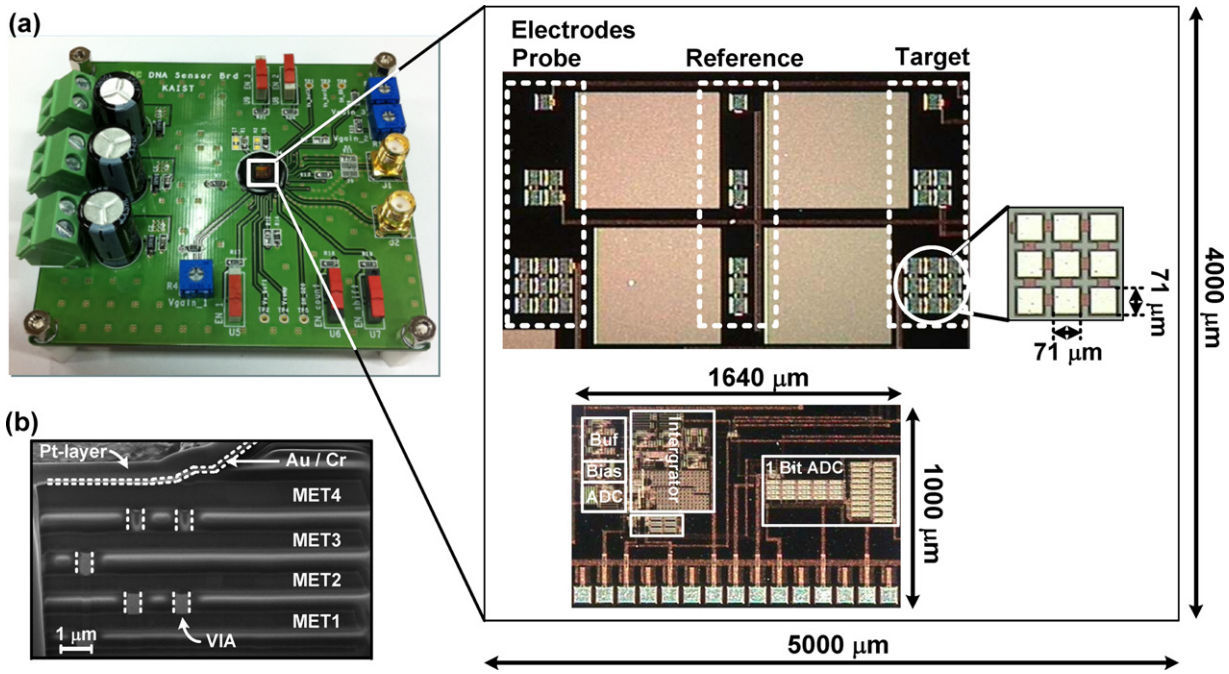

Fig. 3. (a) Schematic of the prototype measurement board and a chip micrograph. The unit electrode has a 71 um square on the surface of the sensor. The total area of the chip is 20 mm^2 and the active area of the readout circuit is 1.64 mm^2. (b) The photo of the chip cross-section after post-fabrication. An Au layer was patterned on a Cr adhesion layer and an exposed Al layer. A Pt layer was used as a protective layer for the FIB (Focused Ion Beam) process.

of the chip was immersed in 10 mM of mercapto hexanol in ethanol for 5 min at room temperature; this process passivates the unreacted electrode surface and reduces the non-specific binding of the probes and the targets. Target DNA strands were hybridized with probes in a 5 × SSC buffer containing 0.1% SDS to reduce the electrostatic repulsion between the probe strands. All impedance measurements were carried out in 0.1 mM PBS (pH 7.4) at room temperature. The low ionic strength level of 0.1 mM was set so that the biomolecular reaction would occur within the Debye length. However, in high ionic strength solutions, the hybridized pair produces a net reduced or even zero charge and thus, no sensor signal can be observed (Poghossian et al., 2005).

3. Results and discussion

3.1. Performance of the designed CMOS sensor

Fig. 4 shows the measured performance from functional operation of the designed biosensor system. Fig. 4(a) shows the target range and the detection limit that the biosensor system can measure. The detectable range was investigated while varying the voltage difference, ΔV ($V_{probe} - V_{target}$), between the two differential electrodes using discrete off-chip components. The accumulation method enlarges the infinitesimal input signal to a readable level while suppressing random noise, resulting in a noise-immune measurement. The sensor achieves a detectable range of 88.3 dB and a detection limit of 36 μV for the surface potential. This performance demonstrates that the proposed device is capable of detecting wide concentrations of targets. Fig. 4(b) shows the operating waveforms of the accumulated signal according to the voltage difference ΔV. The accumulation operates at a speed of 50,000 cycles/s within a predefined window of between 1.45 V and 2.4 V. The accumulation time (t_{acc}) decreases as the difference between the two inputs, V_{probe} and V_{target}, increases. Thus, it is expected that the signal induced by the increased surface charge after hybridization would result in a gradual decrease in the accumulation time.

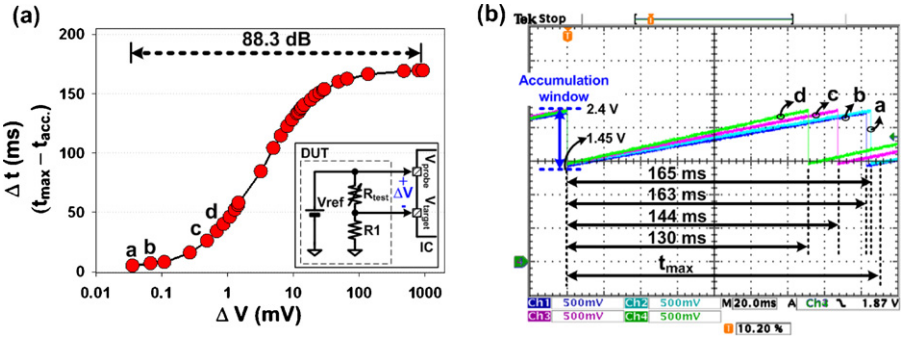

Fig. 4. The measured performance of the designed biosensor in terms of (a) the measurable target range and detection limit, and (b) the operating waveforms. The detectable range was investigated while varying the voltage difference between the two differential electrodes, ΔV ($V_{probe} - V_{target}$) using an off-chip discrete resistor (R_{test}). Additionally, t_{acc} denotes the accumulation time generated at output of integrator by the difference in the input voltages, and t_{max} is the maximum accumulation time under the same inputs, as caused by the mismatched components in the readout circuit. In Fig. 4(b), the waveform 'a' is the accumulating signal when ΔV = 36 μV; 'b' denotes this at ΔV = 68 μV; 'c' at ΔV = 493 μV; and 'd' at ΔV = 875 μV.

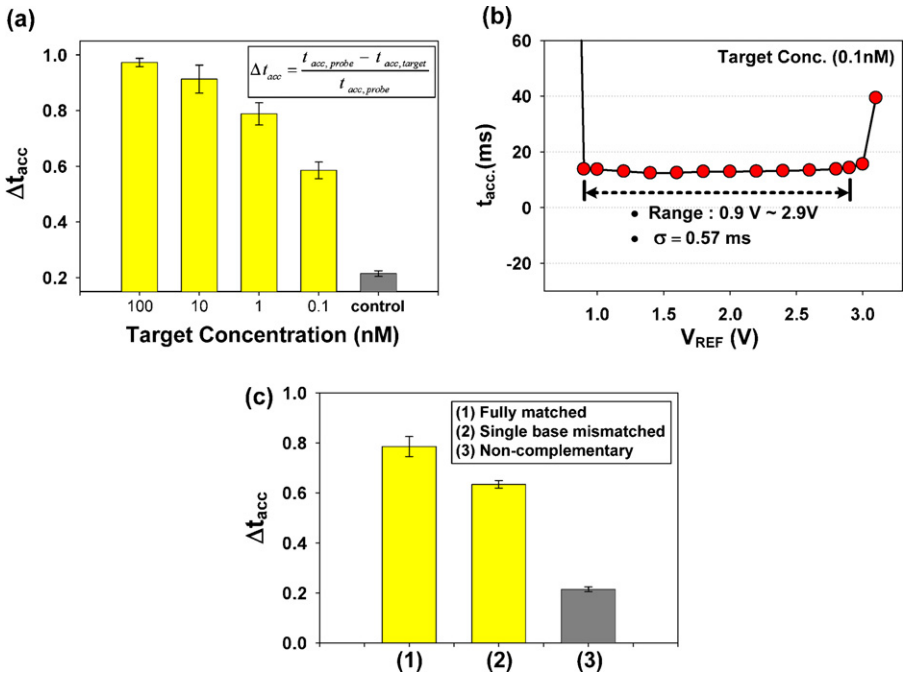

Fig. 5. (a) The measured results of the relative variation of the difference in accumulation time (Δt_{acc}) for hybridization with different target concentrations (100 nM, 10 nM, 1 nM, and 100 pM). The control sample used here was 1 μM of non-complementary DNA. (b) The dependence of the hybridization signal on the reference voltage with a target concentration of 100 pM. Our device shows stable operation while the reference voltage varies in a range of 0.9 V to 2.9 V. (c) Measured result after hybridization with single-base mismatched DNA. (1) 1 nM target DNA (18-mer), (2) single-base mismatched DNA (18-mer), and (3) 1 μM non-complementary DNA.

3.2. Experimental results

In this paper, three conditions required to verify the proposed biosensor system are as follows: (1) an electrode immobilized with probe DNA; (2) an electrode hybridized specifically with complementary DNA strands; and (3) an electrode bound to non-complementary DNA strands. The experiment was carried out by immersing the surface of the electrode in a buffer solution using single-use syringes.

Fig. 5(a) shows the experimental results for the hybridization of the probe DNA and the target DNA with four target oligonucleotide concentrations. The relative variation of the difference in the accumulation time was plotted before and after hybridization of the probe DNA and the target DNA. As expected, the increased surface charge after the hybridization process increases the potential difference between the two differential inputs. The time t_{acc} then decreases. Therefore, the relative variation of the difference in the accumulation time is larger with a high concentration of targets than that with a low concentration of target DNA. The figure shows that specific DNA binding with complementary samples leads to more significant changes compared to that with non-complementary samples. We observed that the induced charge in the working electrode increases as the DNA strand concentration increases. The detection limit of the sensor used in this study was 100 pM, and the normalized variation of the accumulation time changed linearly with the target concentration.

The previous field-effect device, which employs a field-effect modulated by the immobilized molecules on the floating gate of the transistor, has sensitive dependence on the variation of the reference voltage (Bergveld, 1970; Kim et al., 2004). This variation can be caused by a displacement and a polarization of the floating reference electrode, and the variable ionic-strength of the buffer solution from chip to chip. A slight variation of the reference voltage can bring about a large variation of the drain-current or threshold voltage according to the characteristic curve of the transistor. However, Fig. 5(b) shows the dependence of the hybridization signal on the variation of the reference voltage with a target concentration of 100 pM in our device. It is seen that our device achieves stable and robust results over a reference voltage range of 0.9–2.9 V. The standard deviation in the accumulation time in this range is only 0.57 ms. This superior result stems from the differential architecture and direct sensing of the surface potential with

Table 1
Summary of several electrical field-effect devices developed using the intrinsic charges in immobilized molecules.

	This work	Fritz et al. (2002)	Goncalves et al. (2008)	Han et al. (2010)	Maruyama et al. (2009)
Sensor type	CMOS FET with Al plate	Electrolyte–insulator –silicon (EIS) capacitor	Amorphous silicon (a-Si) FET	n-channel FET	CMOS FET with floating gate
Electrolyte; buffer	0.1 mM PBS (pH 7.4)	5 mM sodium phosphate (pH 7.0) 10 mM NaCl	100 mM PBS (pH 7.0)	0.1 × PBS (10 mM, pH 7.4)	PBS (pH 6.86)
Electrode Architecture	Differential	Differential	Single	Single	Single
Target DNA	18-mer ssDNA	12-mer ssDNA	19-mer ssDNA	30-mer ssDNA	22-mer ssDNA
Reference electrode	Built-in Al	Ag/AgCl	Ag/AgCl	N/A	Ag/AgCl
Target DNA concentration	0.1–100 nM	2–80 nM	50 nM	100 nM	25 μM
Readout circuits	Inclusive	Exclusive	Exclusive	Exclusive	Partial inclusive

accumulation method by the device. This independence of the reference voltage makes it possible to choose a wide variety of reference electrode materials.

To demonstrate the specificity of our sensor, we tested whether the device can identify a single-base mismatch in 18-mer oligonucleotides (1 nM). In Fig. 5(c), smaller variation of the difference in the accumulation time from a single-base mismatched sample was observed as compared to a fully matched sample. This demonstrates that our device can successfully differentiate between fully matched complementary and single mismatched DNA sequences. The sequences used in the single-base mismatch test are shown in Supplementary material. These data demonstrate that the proposed biosensor is capable of robustly detecting and quantifying the hybridization of probe and target DNA.

Table 1 presents a summary of several electrical field-effect devices developed using the intrinsic charges in immobilized molecules. Our fully integrated device has good sensitivity and can detect much lower concentrations of target DNA than other FET sensors. It also functions as a better transducer for specific and inexpensive DNA biosensing applications.

4. Conclusion

FET sensors offer label-free and electrical detection when used to quantify the hybridization of DNA strands, thereby allowing rapid, robust and inexpensive measurements. This paper introduced a biosensor based on the direct measurement of the surface potential on bio-modified electrodes using the electrostatic induction of molecular charges. Built-in electrodes and readout circuits were integrated into one package with a standard CMOS process. By repeatedly accumulating the charges that correspond to the surface potential, an improved SNR is achieved in the developed device, through the oversampling effect of accumulation method and the use of a differential architecture. This device uses naked Al as a floating reference electrode without any additional fabrication processes. In addition, our sensor offers stable, robust, and reproducible measurement that is independent of the wide variation of the reference voltage. In this study, a quantitative evaluation of an oligonucleotide derived from an avian influenza on a chip was demonstrated successfully. Our electrical biosensor is thought to have strong potential for use as a bioanalytical tool in point-of-care diagnoses.

Acknowledgments

This work was supported by the National Research Foundation of Korea (NRF) grant funded by the Korea government (MEST) (no. 20110027569). The authors would like to thank J. Huh at the Korea Advanced Institute of Science and Technology for assistance with the mathematical analysis.

Appendix A. Supplementary data

Supplementary data associated with this article can be found, in the online version, at doi:10.1016/j.bios.2011.10.042.

References

Bergveld, P., 1970. IEEE Transactions on Biomedical Engineering 17, 70–71.
Berney, H., West, J., Haefele, E., Alderman, J., Lane, W., Collins, J.K., 2000. Sensors and Actuators B 68, 100–108.
Boon, E.M., Salas, J.E., Barton, J.K., 2002. Nucleic Acid Research 20, 282–286.
Elfstrom, N., Karlstrom, A.E., Linnros, J., 2008. Nano Letters 8, 945–949.
Fritz, J., Cooper, E.B., Gaudet, S., Sorger, P.K., Manalis, S.R., 2002. PNAS 99, 14142–14146.
Goncalves, D., Prazeres, D.M.F., Chu, V., Conde, J.P., 2008. Biosensors and Bioelectronics 24, 545–551.
Han, S.H., Kim, S.K., Park, K., Yi, S.Y., Park, H.J., Lyu, H.K., Kim, M., Chung, B.H., 2010. Analytica Chimica Acta 665, 79–83.
Kricka, L.J., 1999. Clinical Chemistry 45, 453–458.
Kim, D.S., Jeong, Y.T., Park, J.K., Shin, J.K., Choi, P., Lee, J.H., Lim, G., 2004. Biosensors and Bioelectronics 20, 69–74.
Lee, C.S., Kim, S.K., Kim, M., 2009. Sensors 9, 7111–7131.
Lee, K.H., Lee, J.O., Sohn, M.J., Lee, B., Choi, S.H., Kim, S.K., Yoon, J.B., Cho, G.H., 2010. Biosensors and Bioelectronics 26, 1373–1379.
Lee, S.R., Sawada, K., Takao, H., Ishida, M., 2008. Biosensors and Bioelectronics 24, 650–656.
Maruyama, Y., Terao, S., Sawada, K., 2009. Biosensors and Bioelectronics 24, 3108–3112.
Moore, S., 2001. IEEE Spectrum 38, 54–60.
Perkins, F.K., Tender, L.M., Fertig, S.J., Peckerar, M.C., 2002. Proceeding SPIE 4608, 251–265.
Pipper, J., Inoue, M., F-P-Ng, L., Neuzil, P., Zhang, Y., Novak, L., 2007. Nature Medicine 13, 1259–1263.
Poghossian, A., Cherstvy, A., Ingebrandt, S., Offenhausser, A., Schoning, M.J., 2005. Sensors and Actuators B 111–112, 470–480.
Sawada, K., Shimada, T., Ohshina, T., Takao, H., Ishida, M., 2004. Sensors and Actuators B 98, 69–72.
Souteyrand, E., Cloarec, J.P., Martin, J.R., Wilson, C., Lawrence, I., Mikkelson, S., Lawrence, M.F., 1997. Journal of Physical Chemistry B 101, 2980–2985.
Stern, E., Klemic, J.F., Routenberg, D.A., Wyremebak, P.N., Turner-Evans, D.B., Hamilton, A.D., LaVan, D.A., Fahmy, T.M., Reed, M.A., 2007. Nature 445, 519–522.
Werner, O., Harder, T.C., 2006. In: Kamps, B.S., Hoffmann, C., Preiser, W. (Eds.), Influenza Report. Flying Publisher, Paris, pp. 48–86.